Supporting Information for

The Superior Layer-by-Layer Deposition Realizing P-i-N All-Polymer Solar Cells with Efficiency over 16% and Fill Factor over 77%

Qingduan Li,[a,#] Tao Jia,[b,#] Li-Ming Wang,[c,d#] Shengjian Liu,*[,a] Xiaolan Liao,[a] Zhixiong Cao,[a] Jiabin Zhang,[b] Xiaozhi Zhan,[c,d] Tao Zhu,[e] Yue-Peng Cai,[a] Fei Huang*[,b]

[a]School of Chemistry, Laboratory of Polymeric Electronic Materials and Devices, Guangzhou Key Laboratory of Materials for Energy Conversion and Storage, South China Normal University (SCNU), Guangzhou 510006, China

[b]Institute of Polymer Optoelectronic Materials and Devices, State Key Laboratory of Luminescent Materials and Devices, South China University of Technology (SCUT), Guangzhou 510640, China

[c]Spallation Neutron Source Science Center, Dongguan 523803, China[d]Guangdong-Hong Kong-Macao Joint Laboratory for Neutron Scattering Science and Technology, Dongguan 523803, China

[e]Beijing National Laboratory for Condensed Matter Physics and Institute of Physics, Chinese Academy of Sciences, Beijing 100190, China

[#]These authors contribute equally to this work.

Corresponding Authors

***E-mail Addresses:** shengjian.liu@m.scnu.edu.cn (S. Liu), msfhuang@scut.edu.cn (F. Huang)

Content

1. Materials

Solvents including chlorobenzene (CB), chloroform (CF) and 1-chloronaphthalene (CN) were purchased from commercial sources (Aldrich, Alfa Aesar.) and used without further purification unless stated otherwise. Poly(3,4-ethylenedioxythiophene):poly(styrenesulfonate) (PEDOT:PSS, Clevios PVP Al4083 from Heraeus Precious Metals Gmbh & Co. KG). Poly[(2,6-(4,8-bis(5-(2-ethylhexyl)thiophen-2-yl)-benzo[1,2-b:4,5-b′]dithiophene))-alt-(5,5-(1′,3′-di-2-thienyl-5′,7′-bis(2-ethylhexyl)benzo[1′,2′-c:4′,5′-c′]dithiophene-4,8-dione))] (PBDB-T) was purchased from Shanghai Vizuchem. PBDT-TTz and PJ1 were synthesized in our lab. PDINN was purchased from Derthon Co. LTD (Shenzhen, China).

Table S1. Molecular weight and weight distribution of employed polymers used in this work.

Polymer	Mn kDa	Mw kDa	PDI
PBDB-T	92.4	195.9	2.12
PBDT-TTz	153.5	329.9	2.15
PJ1	23.3	39.0	1.67

2. Contact Angle Measurements and Calculation of Flory-Huggins Interaction Parameters

The contact angle tests were performed on a Powereach JC2000C2 Micro surface contact angle analyzer. The surface energy of the polymers was characterized and calculated by the contact angles of the two probe liquids with the Owens and Wendt[1] equation: $(1 + \cos\theta)\gamma_{pl} = 2(\gamma_s^d\gamma_{pl}^d)^{1/2} + 2(\gamma_s^p\gamma_{pl}^p)^{1/2}$, where γ_s and γ_{pl} are the surface energy of the sample and the probe liquid, respectively. The superscripts *d* and *p* refer to the dispersion and polar components of the surface energy, respectively.

Table S2. Dispersion and polar components of the liquid surface free energy (T = 20 ^oC).[2]

Probe liquid	γ_L [mJ m^{-2}]	γ_L^d [mJ m^{-2}]	γ_L^p [mJ m^{-2}]
Water	72.8	21.8	51.0
Hexadecane	27.6	0	27.6

Table S3. Contact angles of water and hexadecane and their parameters for pure polymer donor PBDB-T, PBDT-TTz and pure polymer acceptor PJ1, along with the interaction parameters.

Material	Contact angle (°)		γ	γ_d[a)]	γ_p[a)]	$\chi_{donor,acceptor}$[b)]
	H_2O	Hexadecane	[mN/m]	[mN/m]	[mN/m]	
PBDB-T	102.50 ± 0.29	15.84 ± 0.32	26.95 ± 0.03	26.56 ± 0.03	0.39 ± 0.02	$4.6\times10^{-3}K$
PBDT-TTz	102.95 ± 0.27	20.75 ± 0.29	26.24 ± 0.02	25.84 ± 0.04	0.40 ± 0.01	$1.9\times10^{-2}K$
PJ1	98.90 ± 0.35	13.81 ± 0.37	27.66 ± 0.04	26.81 ± 0.03	0.85 ± 0.02	---

[a)] γ_d and γ_p represent the surface free energies generated from the dispersion forces and the polar forces, respectively, [b)] Flory–Huggins interaction parameter ($\chi_{donor,acceptor}$) was estimated using the equation of $\chi_{donor,acceptor} = K(\sqrt{\gamma_{donor}} - \sqrt{\gamma_{acceptor}})^2$, K is a positive constant.

Table S4. Contact angles of water and hexadecane and their parameters for different materials including polymer donors, polymer acceptors, fullerene derivatives, nonfullerene small molecules.

Material	Contact angle (°)		γ_d [a)]	γ_p [b)]	γ
	H_2O	hexadecane	[mN/m]	[mN/m]	[mN/m]
PBDB-T	102.50	15.84	26.56	0.39	26.95
PBDT-TTz	102.95	20.75	25.84	0.40	26.24
PM6	104.00	18.49	26.19	0.27	26.46
D18	105.87	16.26	26.51	0.11	26.62
N2200	105.01	11.49	27.04	1.14	27.19
PJ1	98.90	13.81	26.80	0.85	27.65
PCBM	94.06	12.20	26.98	1.79	28.77
Y6	98.07	14.34	26.74	1.00	27.74
ITIC	98.64	14.11	26.77	0.88	27.67
IT-2F	97.22	13.56	26.84	1.14	27.98
IT-4F	94.77	11.79	27.02	1.62	28.64
O-ITIC	94.04	13.61	26.83	1.83	28.66

[a), b)] γ_d and γ_p represent the surface free energies generated from the dispersion forces and the polar forces, respectively.

Table S5. Summary of Flory-Huggins intermolecular interaction parameters of donor /acceptor pairs of four polymer donors and eight acceptors including polymer donors, small molecule acceptors and fullerene derivatives.

Donor / Acceptor	PBDT-TTz	PM6	D18	PBDB-T
N2200	$8.5\times10^{-3}K$	$5.0\times10^{-3}K$	$3.0\times10^{-3}K$	$5.3\times10^{-4}K$
PJ1	$1.8\times10^{-2}K$	$1.3\times10^{-2}K$	$9.7\times10^{-3}K$	$4.5\times10^{-3}K$
ITIC	$1.9\times10^{-2}K$	$1.4\times10^{-2}K$	$1.0\times10^{-2}K$	$4.7\times10^{-3}K$
Y6	$2.1\times10^{-2}K$	$1.5\times10^{-2}K$	$1.1\times10^{-2}K$	$5.7\times10^{-3}K$
IT-2F	$2.8\times10^{-2}K$	$2.1\times10^{-2}K$	$1.7\times10^{-2}K$	$9.7\times10^{-3}K$
IT-4F	$5.3\times10^{-2}K$	$4.3\times10^{-2}K$	$3.7\times10^{-2}K$	$2.6\times10^{-2}K$
O-ITIC	$5.3\times10^{-2}K$	$4.4\times10^{-2}K$	$3.8\times10^{-2}K$	$2.6\times10^{-2}K$
PCBM	$5.8\times10^{-2}K$	$4.8\times10^{-2}K$	$4.2\times10^{-2}K$	$3.0\times10^{-2}K$

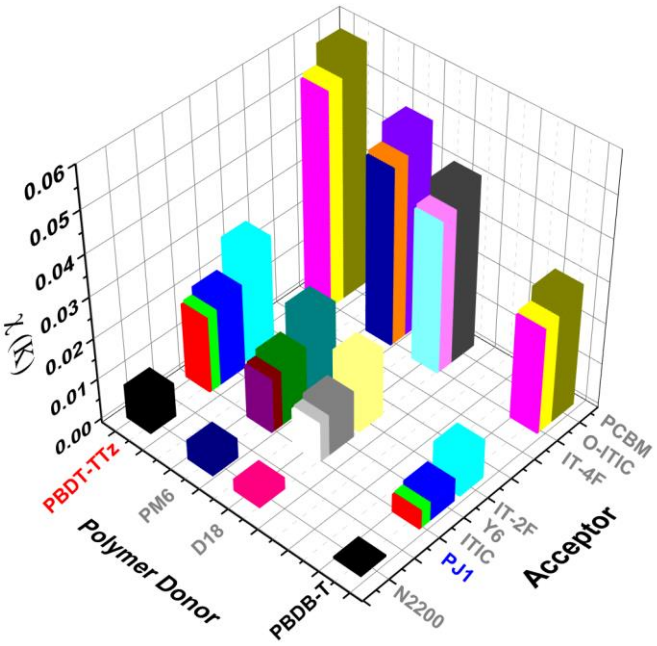

Figure S1. Schematic of Flory-Huggins intermolecular interaction parameters of donor/acceptor pairs of four polymer donors and eight acceptors including polymer donors, small molecule acceptors and fullerene derivatives.

3. Materials Solubility in CN

a) 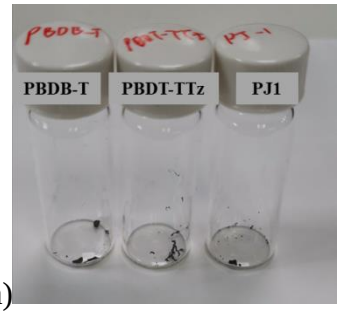

b) 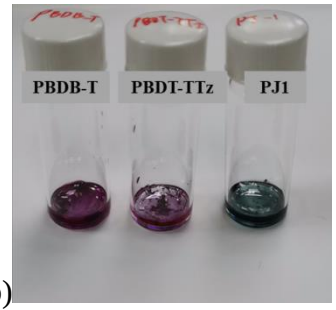

c) 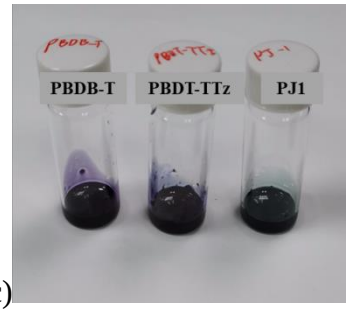

Figure S2. The solubility test of the three polymers PBDB-T, PBDT-TTz and PJ1 in 1-chloronaphthalene (CN) solvent additive; (a) solid materials; (b) materials with freshly added CN; (c) dissolve within 10 min.

4. UV-Vis Solution-Film Spectroscopy

The UV-vis absorption spectra of the polymer or polymer LBL films were obtained on a SHIMADZU UV-3600 spectrophotometer. The sample films for UV-vis absorption measurements were prepared on quartz substrates, and the LBL films were prepared following the same procedures as those for *J*-*V* measurements.

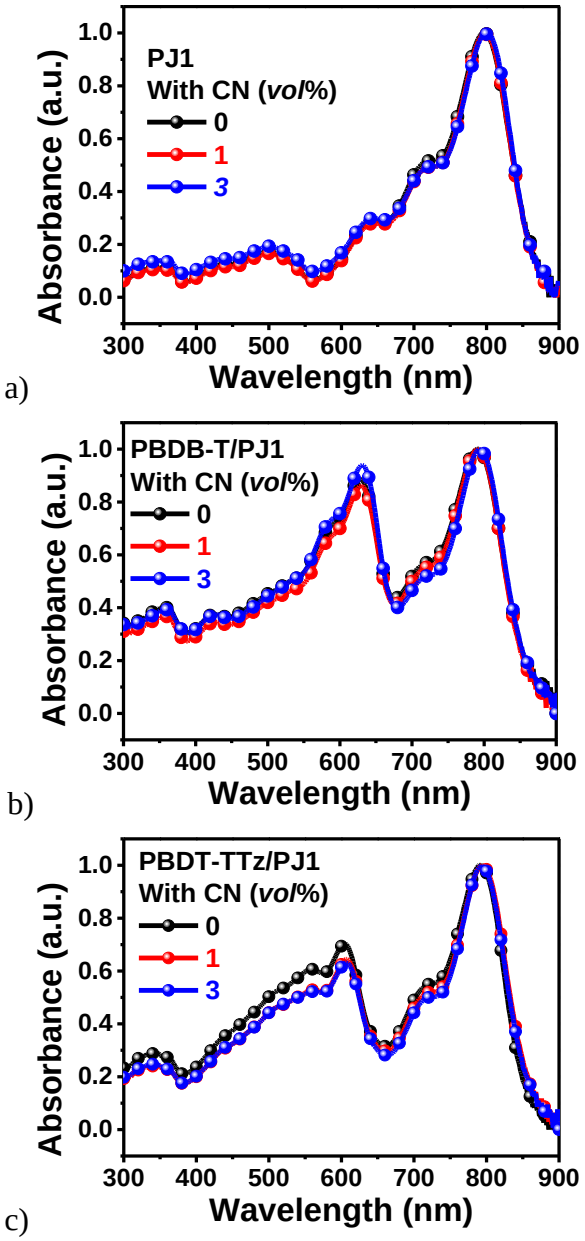

Figure S3. Absorption curves of (a) neat PJ1, (b) PBDB-T/PJ1 LBL films and (c) PBDT-TTz/PJ1 LBL films with different content of CN.

5. Device Fabrication and Characterization

ITO-coated glass substrates were washed using ultrasonic baths by sequentially immersing the substrates in isopropanol once, detergent once, deionized water three times, and isopropanol once, each for 15 min, then baked at 70 ℃ for 3 h in an oven. After that, ITO substrates were treated by UV ozone for 15 min (NovaScan UV Ozone Cleaner), and then poly(3,4-ethylenedioxythiophene):poly(styrenesulfonate) (PEDOT:PSS, Clevios PVP Al4083 from Heraeus Precious Metals Gmbh & Co. KG) was spin-coated onto the precleaned ITO substrates at 3500 rpm for 30 s to obtain ~ 40-nm-thick PEDOT:PSS films. ITO/PEDOT:PSS films were annealed at 150 ℃ for 15 min on a hotplate in atmosphere, and then transferred into a nitrogen-filled glovebox where the active layers were spun atop. The PBDB-T (8 mg/mL), PBDT-TTz (6 mg/mL) were dissolved in CB, and PJ1 (6 mg/mL) was dissolved in CF with 0 *vol*% or other content of CN. For BHJ devices, the active layers were obtained by spin-coating the blend chloroform (CF) solution containing 3 *vol*% CN with the total concentration of 12 mg · mL^{-1}. All the solutions were freshly made and stirred at least 3h before the spin-coating process. The additives were quantitatively added in CF solvent in advance for accuracy. For example, 1 *vol*% CN was obtained by adding 10 μL CN into 990 μL CF solvent. The film thickness was optimized by varying the spin-coating speed of the donor and the acceptor solutions, respectively. The film thickness was determined to be around 105 nm by KLA Tencor P6 surface profilometer. The optimized spin-coating speed for PBDB-T/PJ1 and PBDT-TTz/PJ1 were 1600 rpm/2500 rpm and 1800 rpm/2500 rpm, respectively. The active layers were deposited under vacuum for > 30 min to extract the CN residue before 10 min annealing at 100 ^{o}C. Subsequently, PDINN (1 mg·mL^{-1} in methanol) was solution processed at 3000 rpm. Finally, a 100-nm-thick Ag film was deposited by thermal evaporation at a pressure of < 3×10^{-4} Pa in a glovebox to complete device fabrication.

The characteristic current-voltage (*J*-*V*) curves of the resulting PSCs were measured using a computer-controlled Keithley 2400 sourcemeter under 100 mW cm^{-2} (1 sun, AM 1.5 G spectra, simulator provided by SAN EI, Japan) and using

a mask which has an aperture with precise area of 2 mm × 2 mm (0.04 cm^2) to define the device effective area. The external quantum efficiency (EQE) measurements were carried out by using a QE-R3011 system (Enlitech, Taiwan) from 300 nm to 1000 nm.

6. Additional PV Device Performance Data

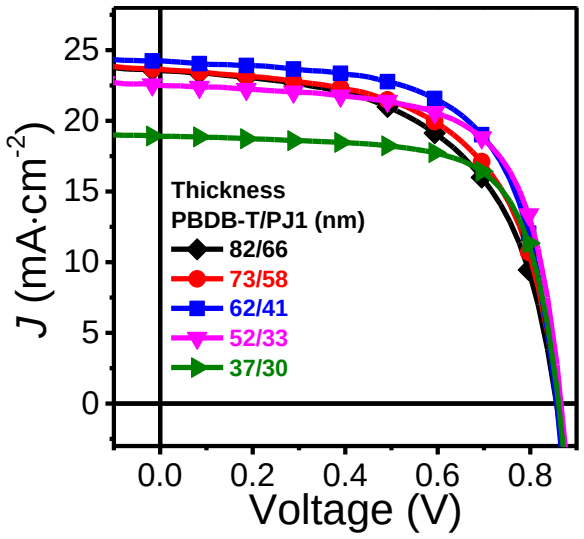

Figure S4. *J-V* curves of PBDB-T/PJ1 LBL without CN devices with different thickness of donor/acceptor active layers under the illumination of AM1.5G, 100 $mW \cdot cm^{-2}$.

Table S6. Photovoltaic performance of as cast PBDB-T/PJ1 LBL devices with different thickness of donor/acceptor active layers under the illumination of AM1.5 G, 100 $mW \cdot cm^{-2}$.[a]

Thickness (nm)	V_{OC} (V)	FF (%)	J_{SC} ($mA \cdot cm^{-2}$)	PCE (%)	
				Best	Average[b]
82/66	0.86	56.9	23.5	11.5	11.3
73/58	0.86	59.4	23.6	12.1	11.7
62/41	0.86	64.1	24.2	13.3	13.1
52/33	0.86	66.8	22.5	13.0	12.7
37/30	0.86	70.0	18.9	11.4	11.3

[a)]Device structure: ITO/PEDOT:PSS/PBDB-T/PJ1/PDINN/Ag; [b)]Average values across >6 devices (device area [mask]: 0.04 cm^2).

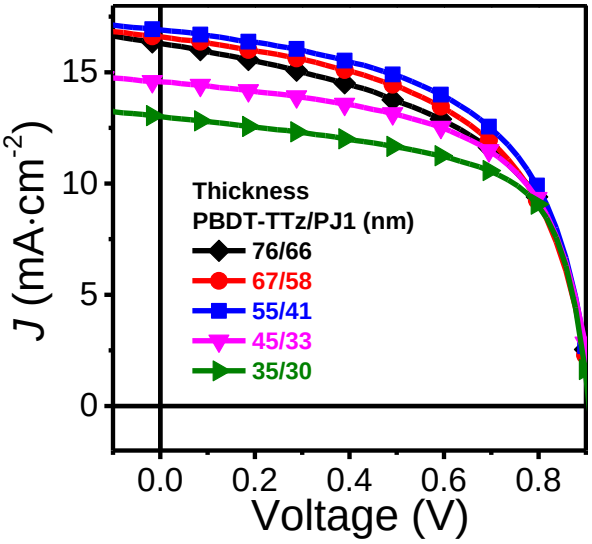

Figure S5. *J-V* curves of PBDT-TTz/PJ1 LBL without CN devices with different thickness of donor/acceptor active layers under the illumination of AM1.5G, 100 $mW \cdot cm^{-2}$.

Table S7. Photovoltaic performance of as cast PBDT-TTz/PJ1 LBL devices with different thickness of donor/acceptor active layers under the illumination of AM1.5 G, 100 $mW \cdot cm^{-2}$.[a]

Thickness (nm)	V_{OC} (V)	FF (%)	J_{SC} ($mA \cdot cm^{-2}$)	PCE (%)	
				Best	Average[b]
76/66	0.92	52.9	16.3	7.9	7.7
67/58	0.92	54.1	16.6	8.2	7.9
55/41	0.92	54.7	16.8	8.5	8.3
45/33	0.92	56.3	15.1	7.8	7.7
35/30	0.92	59.7	13.7	7.5	7.4

[a)]Device structure: ITO/PEDOT:PSS/PBDT-TTz/PJ1/PDINN/Ag; [b)]Average values across >6 devices (device area [mask]: 0.04 cm^2).

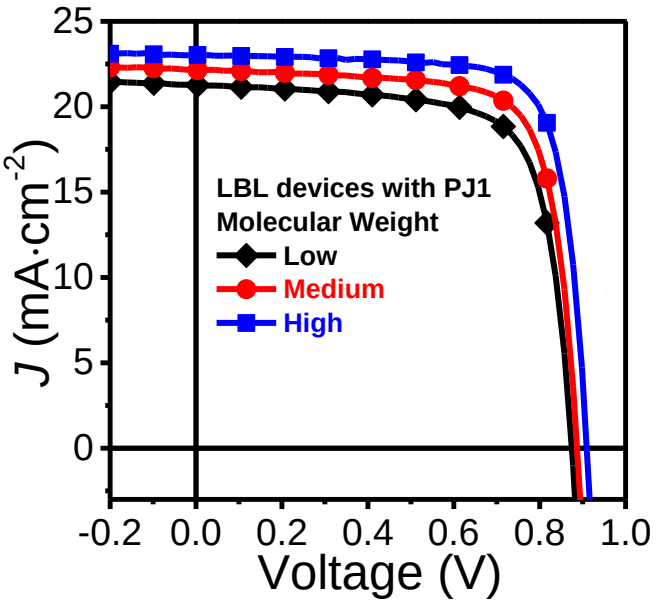

Figure S6. *J-V* curves of CN optimized LBL all-PSCs base PJ1 with different molecular weight.

Table S8. Performance of optimized LBL all-PSCs employed PJ1 with different molecular weight.

PJ1 MW[a)]	PCE (%)	V_{OC} (V)	FF (%)	J_{SC} (mA cm^{-2})
Low	13.5	0.87	72.6	21.3
Medium	14.7	0.89	74.6	22.1
High	16.1	0.90	77.3	23.1

[a)] MW: Molecular Weight

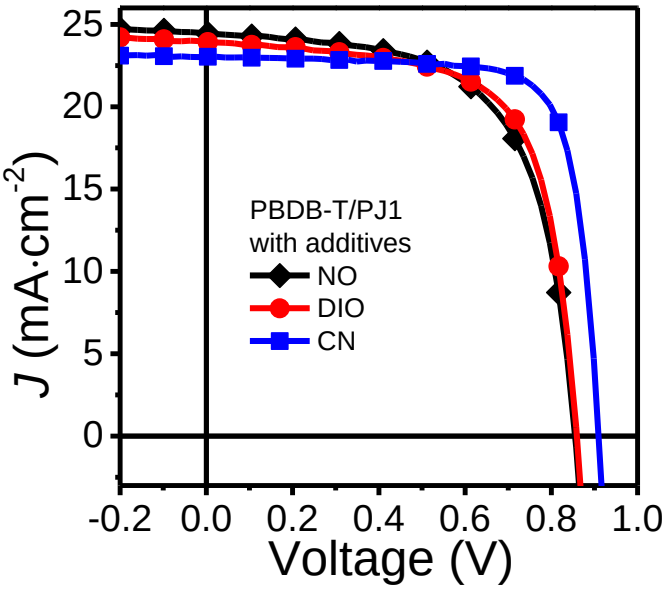

Figure S7. *J-V* curves of PBDB-T/PJ1 LBL devices with different additives

Table S9. Performance of LBL all-PSCs employed different additives.

Additive	PCE (%)	V_{OC} (V)	FF (%)	J_{SC} (mA cm^{-2})
NO	13.2	0.85	63.4	24.4
DIO 1 *vol*%	13.8	0.86	67.2	23.9
CN 1 *vol*%	16.1	0.90	77.3	23.1

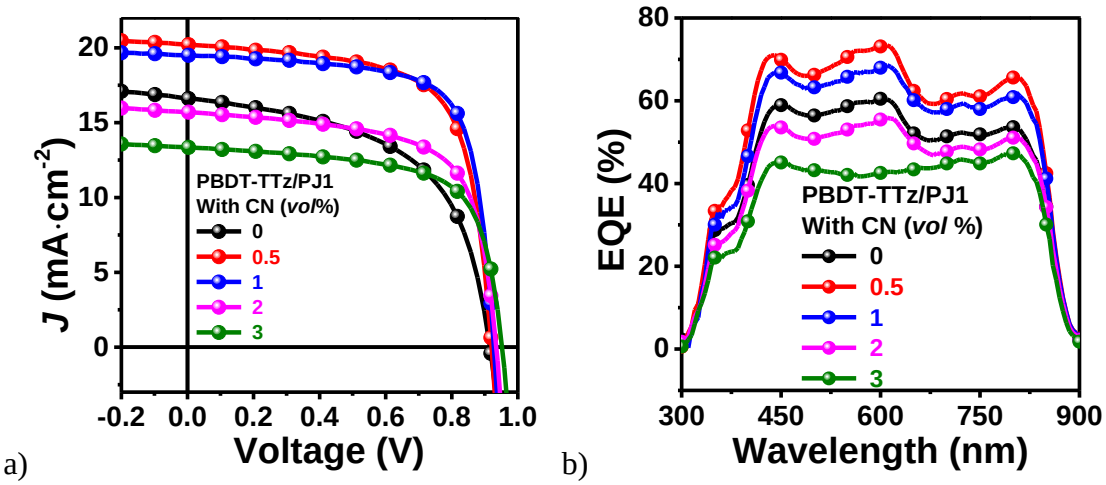

a) b)

Figure S8. *J-V* curves (a) and EQE (b) curves of PBDT-TTz/PJ1 based LBL solar cells with different content of CN.

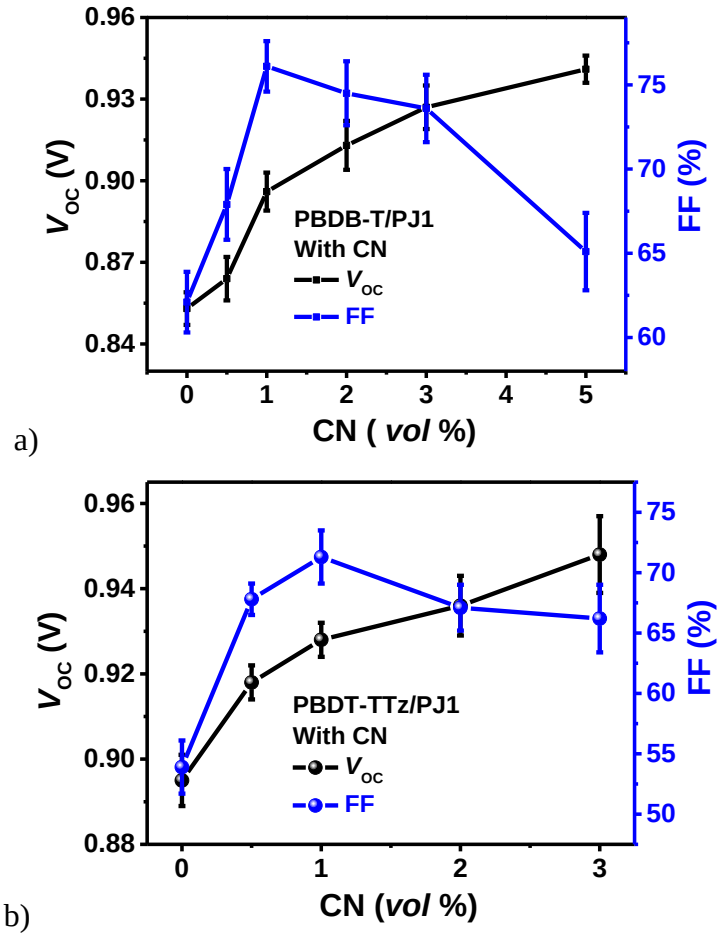

a)

b)

Figure S9. V_{OC} and FF of (a) PBDB-T/PJ1 LBL and (b) PBDT-TTz/PJ1 based LBL all-PSCs as a function of CN content.

Table S10. Photovoltaic parameters of LBL devices based on PBDT-TTz/PJ1 with different content of CN under the illumination of AM1.5, 100 mW cm^{-2}.[a,b]

CN (*vol* %)	PCE (%)	V_{OC} (V)	FF (%)	J_{SC} (mA cm^{-2})	J_{SC} [c] (mA cm^{-2})
0	8.4 (8.2±0.2)	0.91 (0.90±0.1)	54.7 (53.9±2.2)	16.8 (16.5±0.4)	16.6
0.5	12.7 (12.4±0.2)	0.92 (0.92±0.0)	68.2 (67.80±1.3)	20.2 (19.9±0.5)	20.0
1	13.1 (12.8±0.3)	0.93 (0.93±0.0)	71.9 (71.3±2.2)	19.3 (19.1±0.3)	19.0
2	9.9 (9.6±0.2)	0.94 (0.94±0.1)	68.1 (67.1±1.9)	15.7 (15.4±0.4)	15.5
3	8.6 (8.3±0.4)	0.95 (0.95±0.1)	67.5 (66.2±2.8)	13.4 (13.1±0.6)	13.3

[a]Devices were tested under a mask with an area of 0.04 cm^2, [b]Averaged performance with deviation in the brackets from >10 devices, [c] Integrated EQEs are in agreement (±0.5 mA/cm^2; ±4%) with the J_{SC} values reported in Figure S4.

7. Atom Force Microscopy (AFM) Imaging

The nanoscale morphology of blended film was observed using AFM (NT MDT NTEGRA) in the tapping mode. The samples for the AFM measurements were prepared as the same conditions for devices.

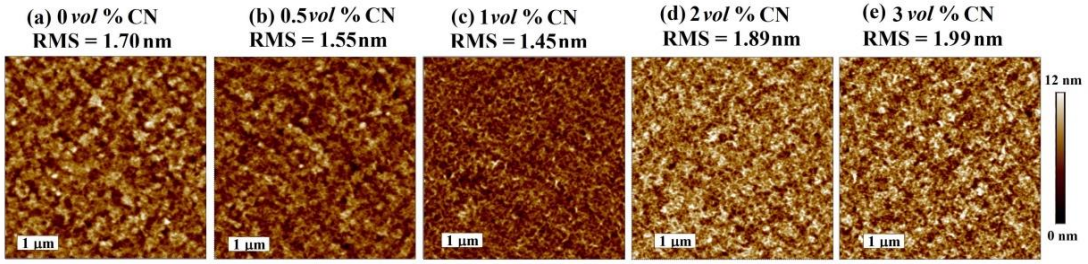

Figure S10. AFM height images (top) and phase images (bottom) of PBDB-T/PJ1 LBL films with different CN ratio (a) 0 *vol*%, (b) 0.5 *vol* %, (c) 1 *vol* %, (d) 2 *vol* %, (e) 3 *vol* %.

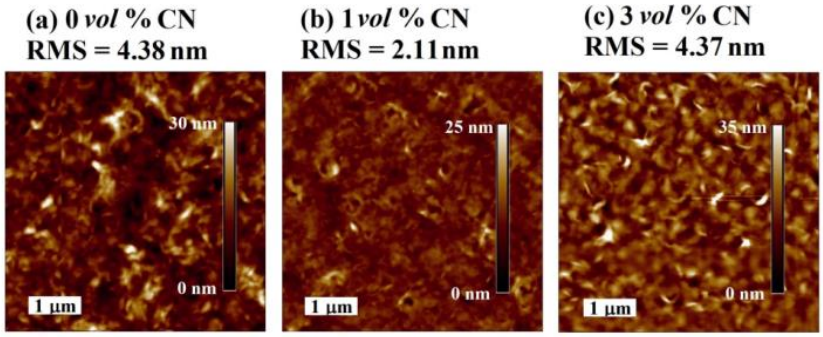

Figure S11. AFM height images of PBDT-TTz/PJ1 LBL films with different CN ratio (a) 0 *vol* %, (b) 1 *vol* %, (c) 3 *vol* %.

8. Contact Angle Measurements of Blend Materials

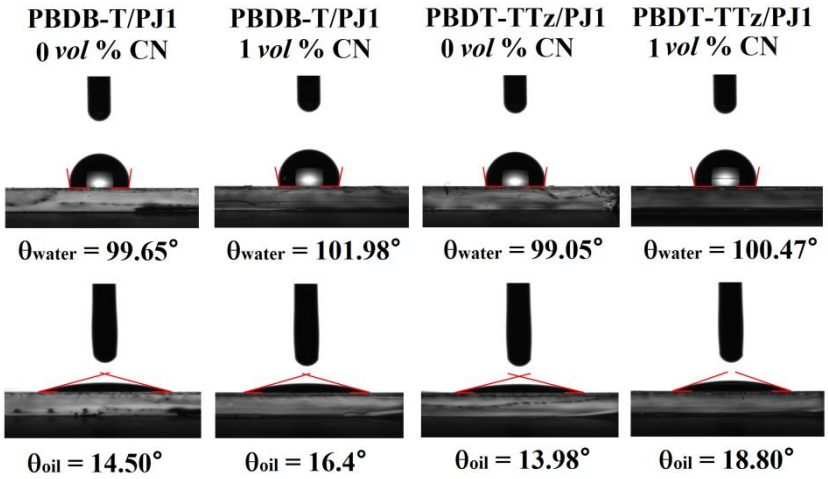

Figure S12. Droplet contact angle images of LBL films (the value in the image is the average contact angle from four tests of different part in the same film.

Table S11. Contact angles of water and hexadecane and their parameters for LBL films of PBDB-T/PJ1 and PBDT-TTz/PJ1 with 0 *vol*% and 1 *vol*% CN along with the SFEs.

LBL Photoactive Layer	Contact angle(°)		γ	γ_d [a)]	γ_p [a)]
	H_2O	Hexadecane	[mN/m]	[mN/m]	[mN/m]
PBDB-T/PJ1 0 *vol*% CN	99.65 ± 0.19	14.50 ± 0.26	27.47 ± 0.03	26.73 ± 0.01	0.74 ± 0.02
PBDB-T/PJ1 1 *vol*% CN	101.98 ± 0.25	16.40 ± 0.16	26.94 ± 0.02	26.49 ± 0.01	0.45 ± 0.01
PBDT-TTz/PJ1 0 *vol*% CN	99.05 ± 0.29	13.98 ± 0.41	27.62 ± 0.03	26.79 ± 0.02	0.83 ± 0.02
PBDT-TTz/PJ1 1 *vol* % CN	100.47 ± 0.32	18.80 ± 0.39	26.83 ± 0.05	26.15 ± 0.03	0.68 ± 0.03

[a)] γ_d and γ_p represent the surface free energies generated from the dispersion forces and the polar forces, respectively.

9. X-ray Photoelectron Spectroscopy (XPS) Measurements

The XPS measurements were performed on Thermo Fisher Scientific (K-ALKPA^{+}) system, A monochromatic Al K_a (1486.68 eV, 12kV) source was employed to generate the excitation and the spectra with a pass energy of 50 eV were finally collected.

Molecular formulas and molecular weight of materials in our work:

- PBDB-T: $(C_{68}H_{80}O_2S_8)_n$, Molecular weight: $(1186)_n$
- PBDT-TTz: $C_{70}H_{92}N_2S_8$, Molecular weight: $(1218)_n$
- PJ1:$C_{121}H_{165}N_8O_2S_6$, Molecular weight: $(1956)_n$

PBDB-T/PJ1 LBL Blend: PBDB-T and PJ1 component ratio could be calculated by S/N ratio.

Make an assumption that the amount of substance of PBDB-T repeat unit on the LBL films surface is ‘a’, and PJ1 repeat unit is ‘b’, so atom ratio of S/N could be described as:

$$(S/N)_{area} = (8a+6b)/8b \qquad (1)$$

Where $(S/N)_{area}$ could be obtained in the XPS results. Donor to acceptor weight ratio is calculated to be 1186a/1956b, the value of a/b could be calculated from equation (1).

PBDT-TTz/PJ1: PBDB-T and PJ1 component ratio could be calculated by S/N ratio.

Make an assumption that the amount of substance of PBDB-T repeat unit on the films surface is ‘a’, and PJ1 repeat unit is ‘b’, then the atom ratio of S/N of PBDT-TTz/PJ1 film could be described as:

$$(S/N)_{area} = (8a + 6b)/(2a+8b) \qquad (2)$$

Where $(S/N)_{area}$ could be obtained in the XPS results. Donor to acceptor weight ratio is calculated to be 1218a/1956b, the value of a/b could be calculated from equation (2).

(b) Carbon contamination at sample surfaces has been taken into consideration in the

XPS measurement. Energy correction based on surface contamination C1s and hydrocarbon C-C peak (284.8 eV) is performed. The evaluation all the atomic ratios are calculated in the XPS measurement in the consideration of sensitivity factors

Table S12. XPS peak intensities of PBDB-T/PJ1 without additives

Name	Start BE	Peak BE	End BE	Height CPS	FWHM eV	Area (P) CPS.eV	Area (N) TPP-2M	Atomic %
C1s	292.46	284.8	278.46	101175.51	1.25	166783.29	2338.7	88.12
O1s	541.26	531.51	525.56	2880.67	2.64	9899.74	57.41	2.16
N1s	406.76	399.32	394.66	4571.38	1.55	12890.66	116.44	4.39
S2p	172.28	163.97	158.68	26879.34	1.21	50992.27	353.05	7.45

Table S13. XPS peak intensities of PBDB-T/PJ1 with 0.5 vol% CN

Name	Start BE	Peak BE	End BE	Height CPS	FWHM eV	Area (P) CPS.eV	Area (N) TPP-2M	Atomic %
C1s	292.69	284.8	278.45	94954.82	1.26	157401.8	2207.15	87.59
O1s	541.25	531.43	525.55	3069.47	2.75	10345.87	60	2.38
N1s	406.75	399.32	394.65	4263.37	1.46	11921.94	107.69	4.27
S2p	171.75	164.21	158.85	9192.36	1.3	19794.39	137.07	5.44

Table S14. XPS peak intensities of PBDB-T/PJ1 with 1 vol% CN

Name	Start BE	Peak BE	End BE	Height CPS	FWHM eV	Area (P) CPS.eV	Area (N) TPP-2M	Atomic %
C1s	292.45	284.8	278.45	99139.85	1.24	157354.71	2206.49	87.63
O1s	541.25	531.13	525.55	3743.75	2.33	11325.44	65.66	2.61
N1s	406.75	399.27	394.65	2625.32	1.55	7232.69	65.33	2.59
S2p	171.75	164.12	158.85	12419.23	1.15	24988.52	173.03	6.87

Table S15. XPS peak intensities of PBDB-T/PJ1 with 2 vol% CN

Name	Start BE	Peak BE	End BE	Height CPS	FWHM eV	Area (P) CPS.eV	Area (N) TPP-2M	Atomic %
C1s	292.58	284.8	278.58	97711.16	1.26	155547.6	2181.14	86.99
O1s	541.38	531.16	525.68	3986.46	2.48	12143.43	70.41	2.81
N1s	406.88	399.21	394.78	2489.21	1.34	6659.4	60.15	2.4
S2p	171.88	164.13	158.98	13849.77	1.1	26953.08	186.63	7.44

Table S16. XPS peak intensities of PBDB-T/PJ1 with 3 vol% CN

Name	Start BE	Peak BE	End BE	Height CPS	FWHM eV	Area (P) CPS.eV	Area (N) TPP-2M	Atomic %
C1s	292.34	284.8	279.14	96802.15	1.27	154968.47	2173.02	86.92
O1s	540.04	531.12	526.14	4341.51	1.51	12851.95	74.51	2.98
N1s	406.24	399.2	394.64	1700.91	1.38	4600.83	41.56	1.66
S2p	170.94	164.16	159.04	14815.34	1.29	28820.09	199.56	7.98

Table S17. XPS peak intensities of PBDT-TTz/PJ1 without CN

Name	Start BE	Peak BE	End BE	Height CPS	FWHM eV	Area (P) CPS.eV	Area (N) TPP-2M	Atomic %
C1s	292.41	284.8	278.71	95840.7	1.28	161578.71	2265.72	86.01
O1s	540.71	532.21	525.91	5256.62	2.38	14936.49	86.67	3.29
N1s	406.81	399.27	394.31	5511.38	1.63	15446.7	139.53	5.3
S2p	171.62	164.22	158.51	7826.81	1.1	16414.2	113.66	4.32

Table S18. XPS peak intensities of PBDT-TTz/PJ1 with 0.5 vol% CN

Name	Start BE	Peak BE	End BE	Height CPS	FWHM eV	Area (P) CPS.eV	Area (N) TPP-2M	Atomic %
C1s	294.33	284.8	280.03	100640.59	1.32	166133.82	2329.59	76.29
N1s	406.33	398.98	395.13	5400.69	1.16	10395.32	157.36	5.15
O1s	539.53	532.16	526.63	4411.74	2.25	12412.8	207.48	6.79
S2p	169.23	164.11	159.43	14277.98	1.16	27581	359.21	11.76

Table S19. XPS peak intensities of PBDT-TTz/PJ1 with 1 vol% CN

Name	Start BE	Peak BE	End BE	Height CPS	FWHM eV	Area (P) CPS.eV	Area (N) TPP-2M	Atomic %
C1s	292.72	284.8	278.92	95461.88	1.3	155059.42	2174.31	85.54
O1s	539.82	532.18	526.12	4621.16	2.18	12388.21	71.88	2.83
N1s	406.22	398.95	393.92	5195.94	1.16	9753.65	88.08	3.47
S2p	171.22	164.11	158.42	13599.01	1.29	27874.51	193.01	7.59

Table S20. XPS peak intensities of PBDT-TTz/PJ1 with 3 vol% CN

Name	Start BE	Peak BE	End BE	Height CPS	FWHM eV	Area (P) CPS.eV	Area (N) TPP-2M	Atomic %
C1s	292.59	284.8	278.59	97748.69	1.29	157979.33	2215.25	85.1
O1s	541.39	532.16	525.69	5629.07	2.15	14565.26	84.51	3.25
N1s	406.89	398.93	394.79	5138.41	1.12	9641.98	87.07	3.34
S2p	171.89	164.08	158.99	14251.55	1.24	28415.17	196.75	7.56

Table S21. Atomic information of LBL films with different CN contents and calculated donor to acceptor weight ratios.

LBL films	CN %	Atomic (%) S	Atomic (%) N	S/N ratio	Acceptor ratio (*wt*%)
PBDB-T/PJ1	0	4.9	4.39	1.12	82
	0.5	5.44	4.27	1.27	76
	1	6.87	2.59	2.65	47
	2	7.44	2.40	3.10	41
	3	7.98	1.66	4.81	29
PBDT-TTz/PJ1	0	4.32	5.30	0.82	95
	0.5	5.81	4.09	1.42	43
	1	7.42	3.47	2.13	35
	3	7.56	3.24	2.33	30

10.Neutron Reflectivity Measurments

All the neutron reflectivity curves were collected from the multipurpose reflectometer (MR, CSNS, China). Reflected neutron were recorded over the wavelength band from 2 Å to 7 Å on a multiwires detector. Data were recorded at three different incident angles (0.3°, 0.6° and 0.8°), three group data sets were integrated to reach a q range from 0.085 $Å^{-1}$ to 0.01 $Å^{-1}$. The collected data were fitted using the GenX reflectometry analysis package,[3] the fitting result reflect the scattering capability of all the atoms in the material to the neutrons, especially on the vertical direction and yields the so called Scattering Length Density (SLD) profile, SLD is defined as the summation of the scattering length and density of each atom, it is written as:

$$\mathrm{SLD} = \sum_j b_j \rho_j \qquad (3)$$

where b_j is the scattering length of the specific atom and ρ_j is the atom number in unit volume, and j runs over all kind of atoms of the layer. Therefore, SLD is able to provide the in-depth component concentration of the blend films.

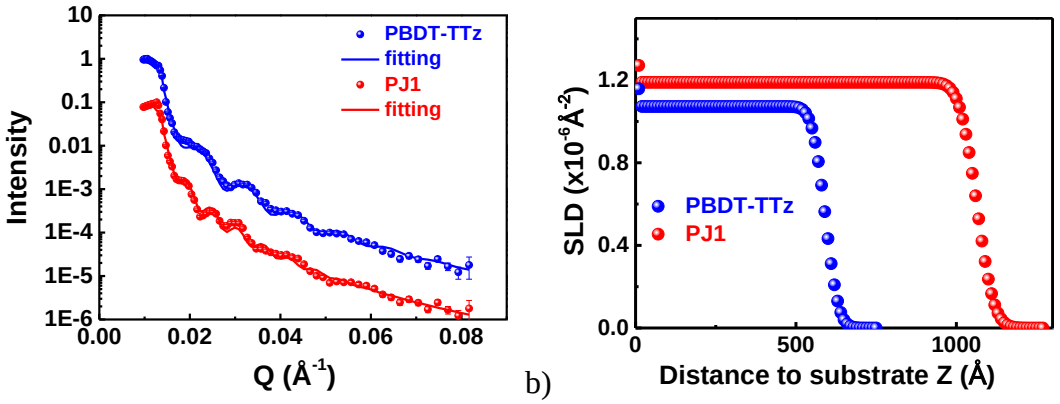

a) b)

Figure S13. (a) Neutron reflectivity profiles for PBDT-TTzand PJ1 thin films. The experimental data are shown as individual points while model fits are shown as lines The traces have been offset for clarity. (b) The corresponding SLD profiles for PBDT-TTz and PJ1 thin films produced by the fittings, respectively.

The SLD of PBDT-TTz and PJ1 are fitted to be 1.07×10^{-6} $Å^{-2}$ and 1.19×10^{-6} $Å^{-2}$ respectively. While the SLD of PBDB-T is referred to the reference.[4]

11.2D Grazing Incidence Wide Angle X-ray Scattering (GIWAXS)

Grazing incidence wide-angle X-ray scattering (GIWAXS) characterization: GIWAXS measurements were performed at beamLine 7.3.3 at the South China University of Technology. The 10 keV X-ray beam was incident at a grazing angle of 0.13^{o}~0.17^{o}, which maximized the scattering intensity from the samples. The scattered X-rays were detected using a Dectris Pilatus 2M photon counting detector.

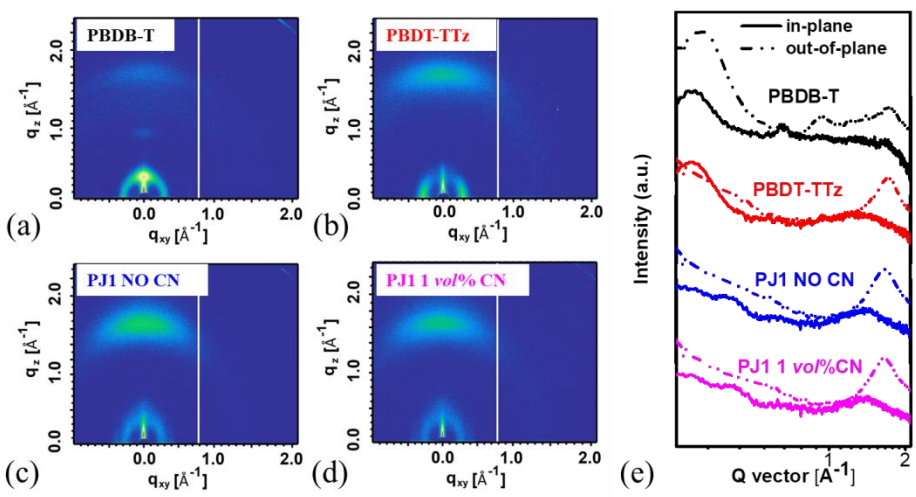

Figure S14. 2D GIWAXS images of (a) neat PBDB-T, (b) neat PBDT-TTz and (c) neat PJ1 and (d) PJ1 with 1 *vol*% CN. And (e) the corresponding the line-cut profiles of the GIWAXS patterns.

Table S22. GIWAXS parameters of PBDB-T, PBDT-TTz, PJ1 and correlated LBL films.

Films	CN (*vol*%)	*q* ($Å^{-1}$)	Distance (Å)	FWHM ($Å^{-1}$)	CCL (Å)
PBDB-T	0	1.71503	3.66	0.30063	18.81
PBDT-TTz	0	1.70885	3.68	0.28142	20.09
PJ1	0	1.66435	3.78	0.31029	18.22
	1	1.65813	3.79	0.3007	18.81
PBDB-T/PJ1	0	1.68239	3.73	0.334	16.93
	1	1.66757	3.75	0.30359	18.63
PBDT-TTz/PJ1	0	1.68203	3.74	0.31017	18.23
	1	1.68033	3.74	0.30553	18.51

12.Photoluminescence (PL) Quenching

Photoluminescence (PL) measurement: PL data were collected using the HORiBA FLUOROMAX-4 fluorimeter. The PL excitation wavelength was set to 610 nm and 800 nm. The sample films for PL measurements were prepared on quartz substrates, and the active layers were prepared using exactly the same concentration and same procedures as those for *J-V* measurements.

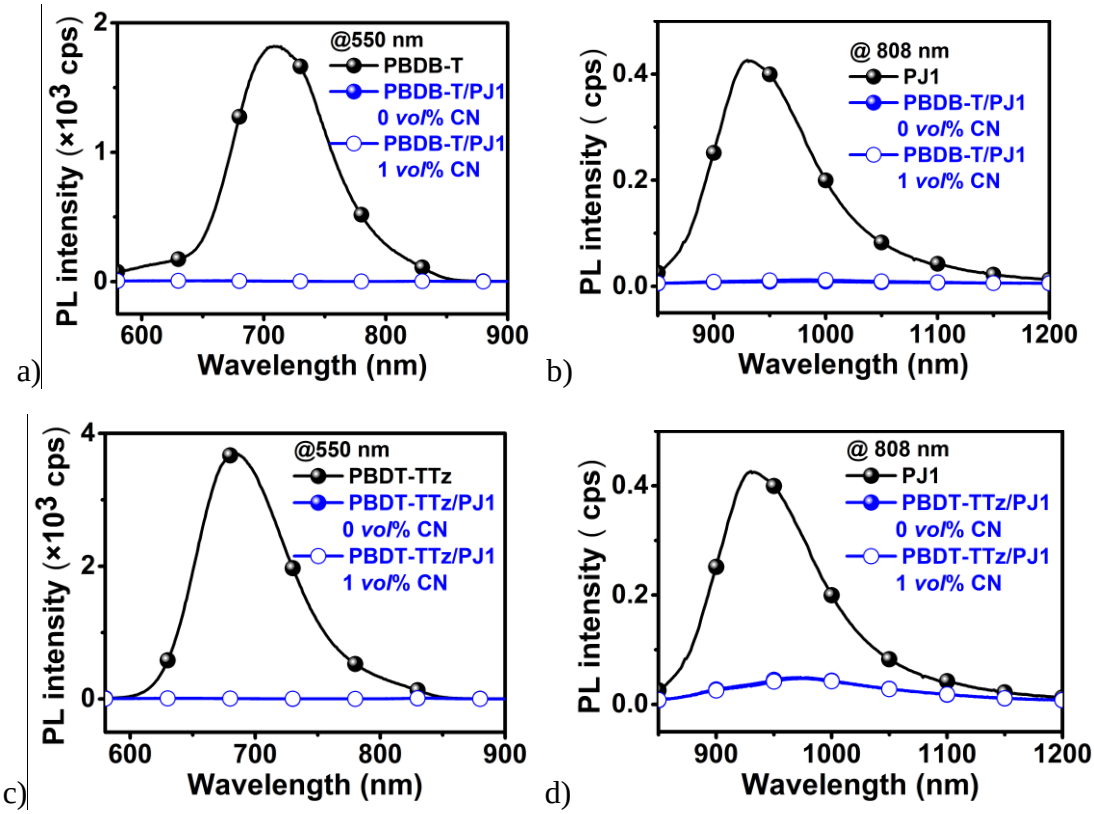

Figure S15. Photoluminescence (PL) quenching of the polymer donors (a) PBDB-T, (b) PBDT-TTz in the presence of PJ1 as in LBL thin films processed with and without optimized CN, with PL quenching efficiency over 95%. Excitation of the polymer donor-rich domains: 550 nm. PL quenching of the acceptor PJ1 in the presence of (c) PBDB-T, (d) PBDT-TTz as in LBL thin films processed with and without optimized CN ratio, PL quenching efficiency over 80%; Excitation of the acceptor Y6-rich domains: 808 nm.

13.Exciton Dissociation and Charge Collection Efficiency

The J_{ph} is calculated by subtracting the dark current density from the current density under illumination, $J_{ph} = J_L - J_D$, where J_L is the current density under illumination and J_D is the dark current density. The V_{int} is defined as $V_{int} = V_0 - V$, where V_0 is the voltage at which J_{ph} equals zero and V is the applied voltage. The V_{int} corresponds to the strength of the electric field amenable to charge carrier extraction.

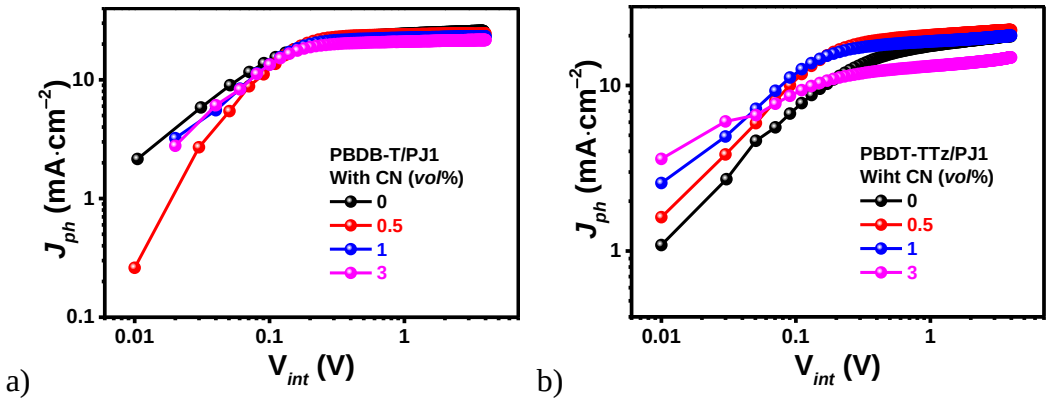

Figure S16. Photocurrent density (J_{ph}) vs. internal voltage (V_{int}) for the LBL devices of PBDB-T/PJ1 and PBDT-TTz/PJ1.

Table S23. Summary of exciton dissociation and charge collection efficiencies of LBL devices with different CN ratio.

Donor	CN (*vol*%)	η_{diss}[a] (%)	η_{coll}[b] (%)	J_{SC} (mA·cm^{-2})	J_{sat} (mA·cm^{-2})	J_{power} (mA·cm^{-2})
PBDB-T/PJ1	0	94.6	76.3	24.3	25.7	19.6
	0.5	98.4	83.7	24.1	24.5	20.5
	1	97.8	88.4	22.7	23.2	20.5
	3	94.0	83.3	20.3	21.6	18.0
PBDT-TTz/PJ1	0	85.9	61.6	17.0	19.8	12.2
	0.5	93.1	77.8	20.1	21.6	16.8
	1	95.5	84.0	19.1	20.0	16.8
	3	90.5	75.5	13.3	14.7	11.1

[a] $\eta_{diss} = J_{SC}/J_{sat}$, [b] $\eta_{coll} = J_{power}/J_{sat}$, J_{sat} is the J_{ph} value at high V_{int} of over 2.0 V, where photogenerated excitons can be dissociated completely into free charge carriers and extracted efficiently by electrodes, and J_{power} is the current intensity at the maximum power point.

14.Fabrication and Characterization of SCLC Devices

Charge mobilities of LBL photoactive layers with CN are estimated from space-charge-limited current (SCLC) method. The device structures of the hole-only and electron-only are ITO/PEDOT:PSS/Active_layer/MoO_3/Ag and ITO/ZnO/Active_layer/PDINO/Ag, respectively. The charge carrier mobilities were estimated by fitting the dark current density according to SCLC equation: $J = (9/8)\varepsilon_r\varepsilon_0\mu(V^2/d^3)$, where J is the current density, μ is the zero-field mobility, ε_0 is the permittivity of free space, ε_r is the relative permittivity of the material, d is the thickness of the active layer, and V is the effective voltage. The effective voltage can be obtained by subtracting the offset voltage (V_{bi}) including built-in voltage and the voltage drop from the series resistance versus the applied voltage (V_{appl}), $V = V_{appl} - V_{bi} - V_s$. The chare mobility was calculated from the slope of the $J^{1/2}$ versus V curves.

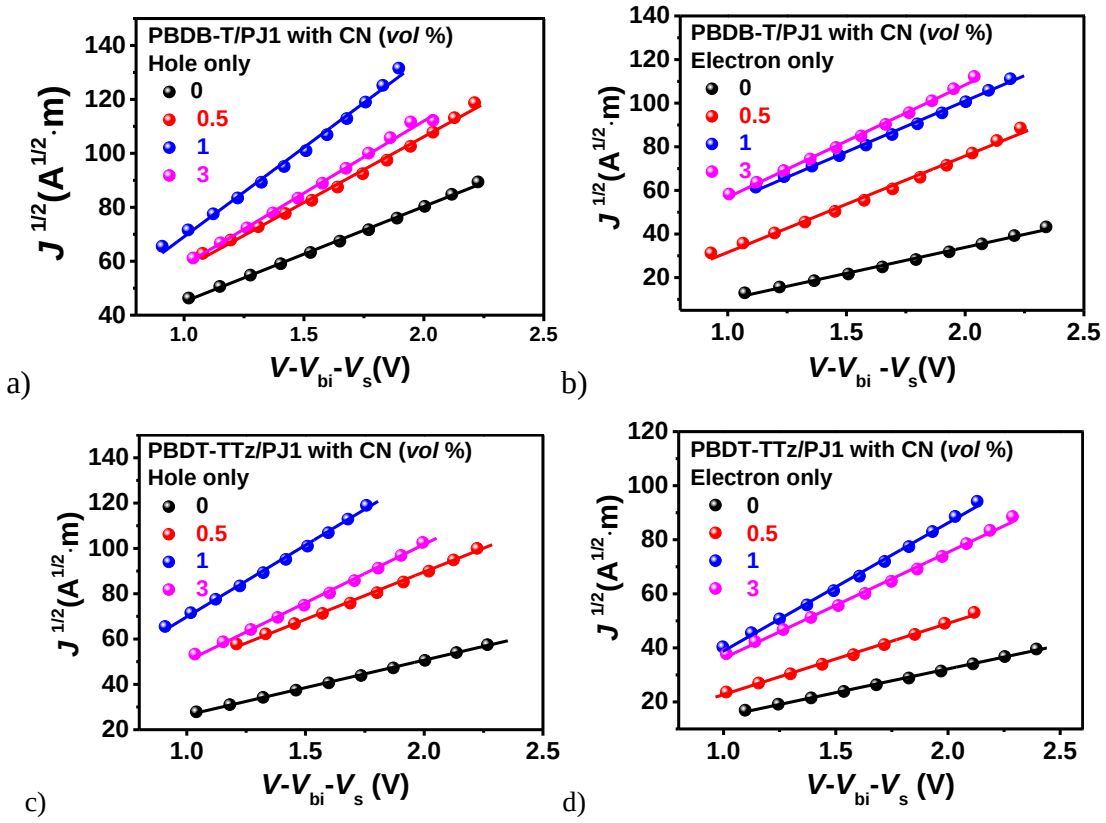

Figure S17. (a), (c) The hole mobility fitting curves for LBL films and (b), (d) the electron mobility fitting curves for LBL films with different CN ratios.

Table S24. Summary of hole and electron mobilities extracted from SCLC fittings shown in Figure S17.

LBL	CN (%)	μ_h ($\times 10^{-4}$ $cm^2 \cdot V^{-1} \cdot s^{-1}$)	μ_e ($\times 10^{-4}$ $cm^2 \cdot V^{-1} \cdot s^{-1}$)	μ_h/μ_e
PBDB-T/PJ1	0	5.5	2.5	2.20
	0.5	10.7	7.5	1.43
	1	15.0	9.4	1.60
	3	13.5	11.6	1.16
PBDT-TTz/PJ1	0	2.0	1.3	1.54
	0.5	6.6	4.6	1.43
	1	14.5	9.8	1.48
	3	10.5	7.1	1.47

15. Charge Recombination

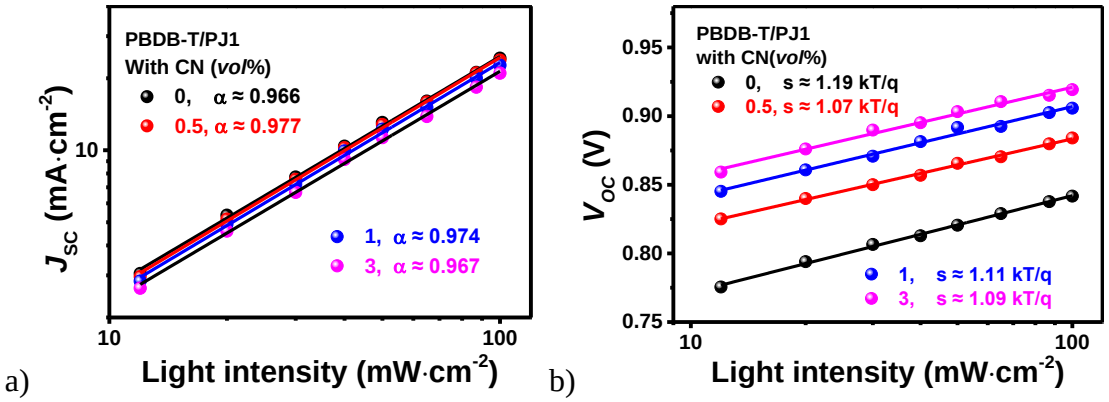

Figure S18. The dependence of (a) J_{SC} and (b) V_{OC} as incident light intensity for the LBL solar devices of PBDB-T/PJ1.

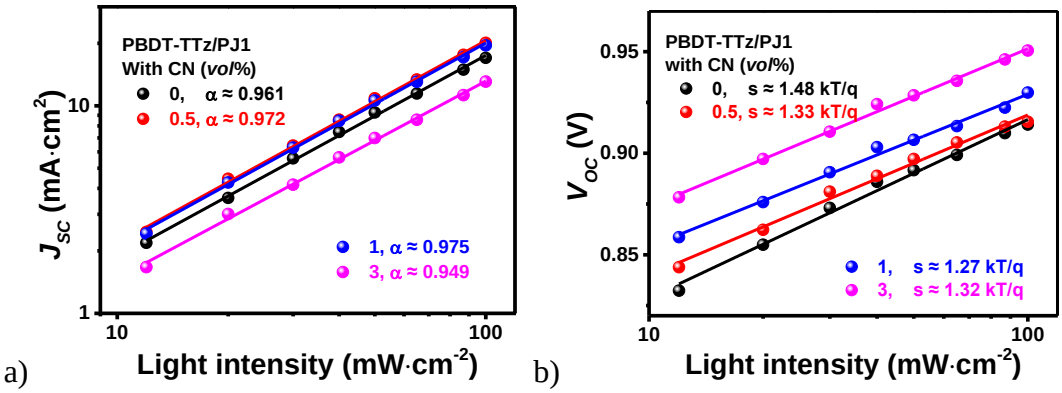

Figure S19. The dependence of (a) J_{SC} and (b) V_{OC} as incident light intensity for the LBL solar devices of PBDT-TTz/PJ1.

16. Supporting Information References

1. D. K. Owens and R. C. Wendt, *J. Appl. Polym. Sci.*, 1969, **13**, 1741-1747.
2. M.-C. Michalski, J. Hardy and B. J. V. Saramago, *J. Colloid Interface Sci.*, 1998, **208**, 319-328.
3. M. Björck and G. Andersson, *J. Appl. Crystallogr.*, 2007, **40**, 1174-1178.
4. Q. Li, L.-M. Wang, S. Liu, X. Zhan, T. Zhu, Z. Cao, H. Lai, J. Zhao, Y. Cai, W. Xie and F. Huang, *ACS Appl. Mater. Interfaces*, 2019, **11**, 45979-45990.